Theoretical Study of Ligand Superhyperfine Structure. Application to Cu(II) Complexes

Frank Neese†

Mathematisch-Naturwissenschaftliche Sektion, Fachbereich Biologie, Universität Konstanz, 78457 Konstanz, Germany

Received: September 13, 2000; In Final Form: February 11, 2001

A theoretical and computational study of the nitrogen superhyperfine structure in Cu(II) complexes is reported. The determination of hybridization parameters for nitrogen donor orbitals from the data is examined. For most Cu(II) complexes the results deviate substantially from pure "sp^2" or "sp^3" hybridization. Semiempirical INDO/S calculations for five Cu(II) complexes were carried out at the UHF and ROHF level. The results suggest that the small anisotropy in the nitrogen hyperfine parameters is caused by spin polarization of the nitrogen valence shell orbitals. A simple, approximate way for the determination of the π-spin density from experimental data is outlined. A density functional study using various basis sets and functionals is reported for the same five complexes. Hybrid functionals, such as B3LYP and PWP1, give better predictions than functionals based on the generalized gradient approximation like BP or BLYP. Provided that at least a polarized triple-ζ basis is used, the hybrid functionals B3LYP and PWP1 give good predictions for the isotropic couplings but overestimate the anisotropic part by almost a factor of 2. The computational results are further analyzed in terms of local versus nonlocal contributions, influence of scalar relativistic and spin−orbit coupling effects and the transferability of quasi-atomic hyperfine couplings.

1. Introduction

Metal−ligand covalency is a key feature in the structure and bonding of transition metal complexes.[1] It is of great importance for many physical and chemical features such as their magnetic and optical properties or their redox potentials. Conversely, physical methods can be used to obtain experimental insight into metal−ligand bond covalencies. Among the most informative techniques are metal and ligand hyperfine couplings (HFCs) in EPR[2] and ENDOR[3] spectra, *g*-values and zero-field splittings,[4] optical transition intensities,[5] and also X-ray spectroscopy.[6] The numbers obtained from the study of ligand-superhyperfine structure, which are perhaps best measured with the ENDOR technique, are thought to be the most accurate because their interpretation appears to be relatively straightforward. In general, this involves an educated guess of reasonably agreed-upon atomic HFCs that are simply scaled to the observed numbers in order to estimate the amount of ligand character mixed in the half-filled metal based molecular orbitals (MOs).

Perhaps the most widely studied systems that show prominent ligand superhyperfine couplings (SHFCs) are complexes of Cu(II) bonded to nitrogen donors in an approximately square planar arrangement.[7] Their magnetic resonance spectra are usually well described by the phenomenological spin Hamiltonian (SH) for $S = {}^1/_2$ that contains terms for the Zeeman energy and the HFC of the unpaired electron with the copper nucleus ($I = {}^3/_2$ for ^{63}Cu and ^{65}Cu)[2]. In addition, it contains terms for the HFC of the unpaired electron with the directly coordinating and possibly also the remote (in the case of imidazole) nitrogen nuclei ($I = 1$ for ^{14}N and $I = {}^1/_2$ for ^{15}N).[2]

Considerable insight into the bonding of the complexes has been obtained by interpreting the SH parameters through molecular orbital theory, as in the classic works of Maki and McGarvey,[8] Kivelson and Neimann,[9] and Ammeter.[10] A schematic MO diagram for a square planar Cu(II) complex in the idealized D_{4h} symmetry group is shown in Figure 1. Both, the ns- and the in-plane np_σ-orbitals of the ligand span the irreducible representations (irreps) $a_{1g}+e_u+b_{1g}$. Of these orbitals, the a_{1g} and b_{1g} fragment orbitals have σ-interactions with the 3d-orbitals of the copper that span the b_{2g} ($3d_{xy}$) + e_g ($3d_{xz}$ and $3d_{yz}$) + a_{1g} ($3d_{z^2}$) + b_{1g} ($3d_{x^2-y^2}$) irreps. The largest overlap occurs between the b_{1g} fragment orbitals and consequently the energetically highest orbital within the copper 3d-derived MOs is the $3b_{1g}$ ("x^2-y^2") MO that according to the Aufbau principle will be the singly occupied MO (SOMO). All π-bonding and π-antibonding MOs are fully occupied and therefore π-donor bonds with the copper ion cannot be formed. Since the square of the SOMO dominates the total spin density, the reason for the nitrogen SHFCs being so prominent in Cu(II) complexes

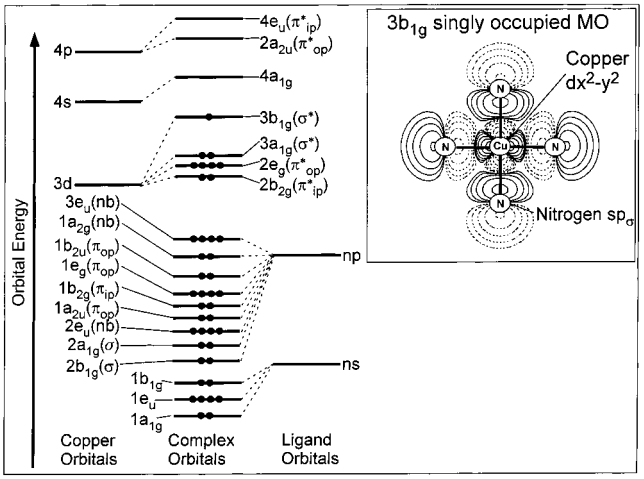

Figure 1. One electron MO scheme for a square planar Cu(II) complex in D_{4h} symmetry. The inset shows the contour plot of the singly occupied MO for a representative complex. Note that depending on the bonding situation of the ligand no or only part of the in-plane (π_{ip}) and out-of-plane (π_{op}) π-orbitals may be available for bonding to the copper (nb = nonbonding in plane orbital).

† E-mail: Frank.Neese@uni-konstanz.de.

10.1021/jp003254f CCC: $20.00
Published on Web 04/07/2001

can be traced back to the fact that the SOMO is strongly σ-antibonding between the metal and the ligand (Figure 1, inset). Thus, the experimental data are directly related to the most covalent MO of such complexes and the numbers obtained from the analysis of the superhyperfine data provide a critical test for any theoretical method that claims to quantitatively model the covalency of metal−ligand bonds.

In recent years first principle electronic structure calculations on transition metal complexes became increasingly feasible due to improvements in the computational algorithms and the hardware.[11] To a large extent they have replaced the older semiempirical models, that still remain useful to quickly rationalize and semiquantitatively predict experimental data. It is known from these studies that Hartree−Fock (HF) theory underestimates the covalencies of metal−ligand bonds due to the improper balance between the exchange and Coulomb contributions to the electron−electron repulsion. Unfortunately, extended correlation treatments are still extremely costly for most transition metal complexes because of their large size and the multiple challenges associated with dynamic and nondynamic correlation effects.[12] Density functional theory (DFT) on the other hand is believed to tend to overestimate the metal−ligand covalencies, at least in the local (local density approximation, LDA) and gradient corrected (generalized gradient approximation, GGA) versions.[13] One motivation for the present work was the speculation that addition of HF exchange in the more recently developed hybrid functionals will correct this deficiency to some extent. We therefore put this hypothesis to a test by applying GGA and hybrid density functionals to the calculation of ligand SHFCs in Cu(II) complexes that, as pointed out above, will be a sensitive indicator of metal−ligand covalency.

Much work has been done on the HFCs in small radicals and organic molecules. Excellent recent reviews on the subject are available.[14] However, much fewer computations have been reported for the interpretation of ligand SHFCs in transition metal complexes. Detailed early work is due to Keijzers and co-workers who correlated high precision experimental data on $[Cu(dtc)_2]$ with extended Hückel calculations.[15,16] Geurts et al.[17] studied the same system using the Hartree−Fock Slater (HFS) method. They evaluated metal- and ligand-SHFC tensors as well as the **g**-tensor using uncoupled Kohn−Sham (KS) perturbation theory and found good agreement between theory and experiment.[17] The most extensive recent work is due to Munzarova and Kaupp, who presented DFT and coupled cluster (CC) results for metal and ligand nuclei in small transition metal containing molecules.[18] The general conclusion reached was that no single functional was able to give uniformly satisfactory agreement with experiment.[18] In particular, the subtle interplay between spin polarization and spin contamination appears to be difficult to model accurately, especially if the HFCs are small and the HFC mechanism is indirect.[18] However, the HFC mechanism studied in the present work is direct and better performance of DFT may be expected. Building on concise earlier work of Watson and Freeman,[19] Munzarova and Kaupp very recently also studied the spin polarization mechanisms responsible for the metal HFCs in detail and significantly enhanced our understanding of these effects.[20] Important contributions to relativistic DFT were made by van Lenthe et al.[21−23] They used the ZORA approach to relativism to study **g**-tensors[22] and HFCs[23] mainly for heavy metal containing systems but also for first row transition metal containing complexes. The relativistic effects (scalar relativistic and spin−orbit coupling) were found to be small for radicals made from light atoms, to be of limited importance for first row transition metals and significant for heavier elements.[23] Using the methodology of Geurts et al.,[17] Belanzoni et al. analyzed the case of TiF_3 in detail and provided considerable insight into the HFC mechanisms of both the metal[24] and the ligand[25] nuclei which even led to the reinterpretation of the experimental spectra.[26] Other DFT studies of ligand SHFCs were also reported.[13b,27]

In this study, a theoretical and computational study of the nitrogen HFCs in Cu(II) complexes will be presented. This work is an indispensable prelude for the application of DFT to the interpretation of large biological and biomimetic Cu(II) systems where the bonding to nitrogen is an important motive and paramagnetic resonance techniques are among the most frequently employed experimental methods. We have avoided to present a study of the metal HFCs in this work as this is a more complicated subject that warrants a separate study.

2. Computational Methods

All DFT hyperfine calculations reported in this work were done with the program system ORCA[28] and were of the spin unrestricted type. The SCF convergence was accelerated with the DIIS method[29] and no particular problems were encountered. Although of questionable theoretical status, it is noted that the $\langle S^2 \rangle$ values for all DFT calculations were in the range 0.75−0.76 which is very close to the value 0.75 expected for spin doublet states.

2.1. Approximate Density Functionals. The B3LYP functional used in this work is defined as in the Gaussian series of programs. The exchange correlation energy is written as

$$E_{XC} = aE_x^{HF} + (1-a)E_x^{LSD} + bE_x^{B88} + cE_c^{LYP} + (1-c)E_c^{VWN} \quad (1)$$

here E_x^{HF} is the HF exchange, E_x^{LSD} is the Slater exchange,[30] E_x^{B88} is Becke's gradient correction to the exchange energy,[31] E_c^{LYP} is the Lee−Yang−Parr (LYP) correlation functional,[32] and E_c^{VWN} is the Vosko−Wilk−Nusair (VWN) parametrization III of the free electron gas correlation energy.[33] Calculations with parametrization V of VWN gave almost indistinguishable results. The parameters *a*, *b* and *c* are those obtained by Becke.[34] The B1LYP functional[35] is formally identical to B3LYP but with parameter values $a = 0.25$, $b = 0.75$, and $c = 1.0$. The BP and BLYP functionals use Becke's gradient corrected exchange and the Perdew[36] or LYP gradient corrected correlation functionals, respectively. The more recently developed PBE functional[37] was also used in both, its pure form (PBE) and as a one parameter hybrid (PBE0, also referred to as PBE1PBE).[38] Here the Perdew−Wang parametrization of the uniform electron gas correlation energy was used.[39] The GP functional uses Gill's gradient corrected exchange[40] together with Perdew's gradient corrected correlation functional. Finally, the PWP and PWP1 functionals use the Perdew−Wang gradient corrected exchange[41] together with Perdew's gradient corrected correlation functional. PWP1 refers to the one parameter hybrid version (formally $a = 0.25$, $b = 0.75$, and $c = 1.0$) of this functional.

2.2. Basis Sets.[42] HFC calculations are known for having rather stringent basis set requirements, especially in the core region.[14,18,23] We have therefore studied basis set effects and fully documented the results in the Supporting Information (Table S1). The basis set that provides a reasonable compromise between efficiency and accuracy, and that was used for all calculations reported in this paper, is based on the polarized triple-ζ (TZVP) basis set of Schäfer et al.[43] for the metal and

the nitrogen ligands, while all other atoms are treated with the DZVP basis of Godbout et al.[44] The only enhancement relative to the standard TZVP basis set that proved to be necessary was to decontract the innermost and outermost primitives in the 1s basis function of the nitrogen atoms in order to provide sufficient flexibility in the core region. Addition of multiple sets of polarization functions on all atoms did not change the results to any significant extent.

The convergence with respect to the numerical integration accuracy of the DFT procedure was also studied and it was concluded that the results reported here are converged to better than 0.1 MHz.

2.3. Relativistic Calculations. A limited set of calculations including relativistic corrections were carried out with the ADF 1999 program.[45] In these calculations, the ZORA approach[21−23] was used together with the all electron Slater type orbital (STO) ADF basis set IV that was optimized for ZORA calculations. This basis set is of triple-ζ plus polarization quality in the valence region and contains additional steep functions in the core region. The BP functional has been employed in these calculations. Note that slight differences between ADF 1999 and ORCA may be caused by the fact that the ADF program uses the VWN V parametrization[33] of the uniform electron gas as the underlying LDA while ORCA uses the Perdew-Wang parametrization[39] in conjunction with the BP functional.

2.4. Geometries. For $[Cu(NH_3)_4]^{2+}$ the Cu−N bond length 2.05 Å and a square planar arrangement was assumed on the basis of the crystal structures of several salts containing this unit.[46] The geometries of the other complexes were first optimized with the BPW91 functional and the DZVP basis set using the DGauss program[51] and no symmetry constraints. For $[Cu(iz)_4]^{2+}$ a Cu−N distance of 2.028 Å was computed compared to the average Cu−N distance of 2.010 Å found experimentally for Tetrakis(imidazole)dinitratocopper(II).[47] For $[Cu(py)_2]^{2+}$ the computed Cu−N distance is 2.047 Å compared to the average experimental value of 2.027 Å obtained for the perchlorate salt.[48] The complexes $[Cu(en)_2]^{2+}$ and $[Cu(gly)_2]$ were further optimized with the TurboMole program system[52] under C_2 and C_{2v} symmetry constraints, respectively. The B3LYP method and a TZVP basis set was used. The resulting metal−ligand bond length for $[Cu(en)_2]^{2+}$ was 2.067 Å in moderate agreement with the average X-ray diffraction value of 2.015 Å obtained for the perchlorate salt.[49] For $Cu(gly)_2$ the agreement with the crystal structure of the monohydrate[50] was also moderate. The calculated bond lengths were $R(Cu-O) =$ 1.910 Å and $R(Cu-N) = 2.041$ Å compared to 1.952 and 2.001 Å found experimentally.

The dependence of the computed HFCs on the copper−nitrogen distance was carefully studied for the case of $[Cu(NH_3)_4]^{2+}$ and the results are documented in the Supporting Information, Table S2. The observed variations were dominated by changes in the isotropic HFC. Within a range of 0.05 Å, the variation of the HFCs were on the order of 2−3 MHz. Therefore, the errors in the computed geometries will not have a major influence on the results reported below.

2.5. Hyperfine Calculations. The hyperfine tensors were calculated by direct analytical integration over the chosen basis set and using the self-consistent DFT spin density. Algorithms for the calculation of field gradient integrals over Gaussian basis functions have been reported by McMurchie and Davidson[53] and were authoritatively reviewed by Helgaker and Taylor.[54] For the constant factor $g_e g_N(^{14}N)\beta_e\beta_N$ the value 38.567 MHz bohr^3 was used. Our implementation into ORCA was verified by comparing the calculated isotropic and anisotropic HFCs for several small molecules between the Gaussian98W[55] (Prop = EPR) and ORCA programs using identical geometries, basis sets and DFT functionals.

2.6. Semiempirical Calculations. Semiempirical calculations were also done with the program ORCA and the INDO/S method of Zerner and co-workers.[67] In preliminary work it was found that the parameter $\beta(Cu)$ should be set to −20 eV in order to get good spectral predictions for Cu(II) complexes.[56] In keeping with the philosophy of the ZDO approach, that implicitly refers to a symmetrically orthogonalized basis set, only the one-center integrals were retained in the hyperfine calculations. The atomic parameters were 1540 MHz for $A_{iso}^{^{14}N}$ and 116.5 MHz for $g_e\beta_e g(^{14}N)\beta_N\langle r^{-3}\rangle_{2p}$. The latter value was calculated from the value 3.01988 au^{-3} for $\langle r^{-3}\rangle_{2p}$[66] and the former from the value 4.770 au^{-3} for $|\psi_{2s}(0)|^2$.[57] No attempt was made to change these values in order to improve the agreement with experimental HFCs.

3. Theory

The phenomenological SH that describes the magnetic resonance spectra of square-planar Cu(II) complexes is[2]

$$\hat{H}_{spin} = \beta B g_{\|}\hat{S}_z + \beta B g_{\perp}(\hat{S}_x + \hat{S}_y) + A_{\|}^{Cu}\hat{S}_z\hat{I}_z^{Cu} + A_{\perp}^{Cu}(\hat{S}_x\hat{I}_x^{Cu} + \hat{S}_y\hat{I}_y^{Cu}) + \sum_{N_i}\hat{S}\mathbf{A}(N_i)\hat{I}^{N_i} \quad (2)$$

where $g_{\|}$ and $g_{\perp}$ are the elements of the **g**-matrix, $A_{\|}^{Cu}$ and $A_{\perp}^{Cu}$ are the principle values of the copper HFC, $\mathbf{A}(N_i)$ is the HFC tensor for the ith nitrogen ligand, $\hat{S}$ is the operator for the fictitous electron spin, and the $\hat{I}$'s are nuclear spin operators. B is the magnetic flux density and β is Bohr's magneton. The theoretical challenge is to provide a microscopic theoretical treatment that predicts the parameters in eq 2 based on the molecular geometric and electronic structure. In this work the focus is on the nitrogen HFC tensor $\mathbf{A}(N_i)$.

Consider the ground state of the Cu(II) complex under consideration which may be described by a many electron wave function Ψ_S^M. As explained for example by McWeeny,[58] the HFC is related to the normalized spin density function:

$$D_s(\vec{r}) = \frac{1}{2M}[P_1^{\alpha}(\vec{r}) - P_1^{\beta}(\vec{r})] \quad (3)$$

by the relation ($P_1^{\alpha}(r)$ and $P_1^{\beta}(r)$ are the one-electron densities for spin-up and spin-down electrons):

$$\mathbf{A}(N_i) = A^{iso}(N_i)\,\mathbf{1} + \mathbf{A}^{dip}(N_i) + \mathbf{A}^{orb}(N_i) \quad (4a)$$

$$A^{iso}(N_i) = \frac{8\pi}{3}P_N D_S(\vec{R}_{N_i}) \quad (4b)$$

$$A_{ij}^{dip}(N_i) = P_N\int\hat{F}_{ij}(N_i)D_S(\vec{r})d^3r \quad (4c)$$

where $P_N = \beta_e\beta_N g_e g(^{14}N)$ and the dipole−dipole interaction operator at center N_i can be represented by

$$\hat{F}_{ij}(N_i) = \frac{\partial}{\partial\vec{r}_i}\frac{\partial}{\partial\vec{r}_j}\frac{1}{|\vec{r} - R_{N_i}|} \quad (5)$$

$\mathbf{A}^{orb}(N_i)$ is a second-order correction[15a] that is assumed to be negligible in this section. Further evidence for this assumption will be presented in section 4.2.4 where this term is explicitly calculated. If the density is expressed in terms of a set of fixed, atom-centered basis functions $\{\varphi\}$, D_s can be written as[58]

$$D_s(\vec{r}) = \sum_{A,B}\sum_{k,l}\rho_{kl}\varphi_k^A(\vec{r})\varphi_l^B(\vec{r}) \quad (6)$$

where φ_k^A is the kth basis function centered on atom A and ρ_{kl} is an element of the spin-density matrix ($\rho_{kl} = P_{kl}^a - P_{kl}^\beta$). The hyperfine tensor for a nitrogen ligand can be decomposed into several parts:

$$A^{\mathrm{iso}}(\mathrm{N}_i) = A_{\mathrm{loc}}(\mathrm{N}_i) + A_{\mathrm{nonloc}}(\mathrm{N}_i) \quad (7a)$$

$$\mathbf{A}^{\mathrm{dip}}(\mathrm{N}_i) = \mathbf{A}_{\mathrm{dip}}^{1-\mathrm{center}}(\mathrm{N}_i) + \mathbf{A}_{\mathrm{dip}}^{2-\mathrm{center}}(\mathrm{N}_i) + \mathbf{A}_{\mathrm{dip}}^{3-\mathrm{center}}(\mathrm{N}_i) \quad (7b)$$

The local contribution to the isotropic HFC arises from the spin density in the s-orbitals on atom N_i. The nonlocal correction to the isotropic HFC divides into two parts:

$$A_{\mathrm{nonloc}}(\mathrm{N}_i) = A^{nl;\mathrm{cf}}(\mathrm{N}_i) + A^{nl;\mathrm{bond}}(\mathrm{N}_i) \quad (8)$$

$$A^{nl;cf}(\mathrm{N}_i) = \frac{8\pi}{3}P_{\mathrm{N}}\sum_{A\neq\mathrm{N}_i}\sum_{B\neq\mathrm{N}_i}\sum_k^A\sum_l^B \rho_{kl}\varphi_{\mathrm{k}}^{\mathrm{A}}(\vec{R}_{\mathrm{N}_i})\varphi_l^{\mathrm{B}}(\vec{R}_{\mathrm{N}_i}) \quad (8a)$$

$$A^{nl;\mathrm{bond}}(\mathrm{N}_i) = \frac{16\pi}{3}P_{\mathrm{N}}\sum_{A\neq\mathrm{N}_i}\sum_k^A\sum_l^{\mathrm{N}_i} \rho_{kl}\varphi_{\mathrm{k}}^{\mathrm{A}}(\vec{R}_{\mathrm{N}_i})\varphi_l^{\mathrm{B}}(\vec{R}_{\mathrm{N}_i}) \quad (8b)$$

The superscript on the summation indicates that the sum includes only the basis functions that belong to the indicated atom. The nonlocal part is further divided into a "crystal-field" contributing basis functions are on neighboring atoms and a 'bond' contribution, where only one function is located on another center. The two-center corrections to the first-order anisotropic part of the nitrogen HFC also divide into "crystal-field" and "bond" contributions:

$$\mathbf{A}_{\mathrm{dip}}^{2-\mathrm{center}}(\mathrm{N}_i) = \mathbf{A}_{\mathrm{dip}}^{2-\mathrm{center:cf}}(\mathrm{N}_i) + \mathbf{A}_{\mathrm{dip}}^{2-\mathrm{center;bond}}(\mathrm{N}_i) \quad (9)$$

where,

$$\mathbf{A}_{\mathrm{dip}}^{2-\mathrm{center:cf}}(\mathrm{N}_i) = P_{\mathrm{N}}\sum_{A\neq\mathrm{N}_i}\sum_k^A\sum_l^A \rho_{kl}\langle\varphi_k^A|\hat{\mathbf{F}}(\mathrm{N}_i)|\varphi_l^A\rangle \quad (9a)$$

$$\mathbf{A}_{\mathrm{dip}}^{2-\mathrm{center;bond}}(\mathrm{N}_i) = 2P_{\mathrm{N}}\sum_{A\neq\mathrm{N}_i}\sum_k^A\sum_l^{\mathrm{N}_i} \rho_{kl}\langle\varphi_k^A|\hat{\mathbf{F}}(\mathrm{N}_i)|\varphi_l^A\rangle \quad (9b)$$

The "crystal-field" contribution arises from the spin located at remote atoms. At large distances this term can be presented by a point-dipole approximation.[3,59] The "bond" contribution arises from the unpaired spin density in the bonds surrounding atom N_i. Finally, the three-center terms arise from the spin density in remote bonds and are given by

$$\mathbf{A}_{\mathrm{dip}}^{3-\mathrm{center}}(\mathrm{N}_i) = P_{\mathrm{N}}\sum_{A\neq\mathrm{N}_i}\sum_{B\neq\mathrm{N}_i}\sum_k^A\sum_l^B \rho_{kl}\langle\varphi_k^A|\hat{\mathbf{F}}(\mathrm{N}_i)|\varphi_l^A\rangle \quad (10)$$

A similar partitioning has been carried out before by Keijzers and Snaathorst and the individual terms were evaluated with STO-6G fits to extended Hückel orbitals for $[Cu(dtc)_2]$.[15d] In this section A_{nonloc}, $\mathbf{A}_{\mathrm{dip}}^{2-\mathrm{center}}$, $\mathbf{A}_{\mathrm{dip}}^{3-\mathrm{center}}$, and $\mathbf{A}^{\mathrm{orb}}$ are assumed to be small corrections that will be neglected. In sections 4.2.4 and 4.2.3 they will be directly evaluated from DFT calculations.

If the symmetry of the complex is sufficiently high, such that the off-diagonal elements of the spin density matrix can be neglected, one obtains for the nitrogen HFCs

$$A_\sigma(\mathrm{N}_i) = A^{\mathrm{iso}}(\mathrm{N}_i) + P_{\mathrm{N}}\langle r^{-3}\rangle_{\mathrm{N2p}}\left(\frac{4}{5}\rho_\sigma^{\mathrm{N}_i} - \frac{2}{5}\rho_{\pi_{ip}}^{\mathrm{N}_i} - \frac{2}{5}\rho_{\pi_{op}}^{\mathrm{N}_i}\right) \quad (11a)$$

$$A_{\pi_{\mathrm{ip}}}(\mathrm{N}_i) = A^{\mathrm{iso}}(\mathrm{N}_i) + P_{\mathrm{N}}\langle r^{-3}\rangle_{\mathrm{N2p}}\left(-\frac{2}{5}\rho_\sigma^{\mathrm{N}_i} + \frac{4}{5}\rho_{\pi_{\mathrm{ip}}}^{\mathrm{N}_i} - \frac{2}{5}\rho_{\pi_{\mathrm{op}}}^{\mathrm{N}_i}\right) \quad (11b)$$

$$A_{\pi_{\mathrm{op}}}(\mathrm{N}_i) = A^{\mathrm{iso}}(\mathrm{N}_i) + P_{\mathrm{N}}\langle r^{-3}\rangle_{\mathrm{N2p}}\left(-\frac{2}{5}\rho_\sigma^{\mathrm{N}_i} - \frac{2}{5}\rho_{\pi_{\mathrm{ip}}}^{\mathrm{N}_i} + \frac{4}{5}\rho_{\pi_{\mathrm{op}}}^{\mathrm{N}_i}\right) \quad (11c)$$

$$A_{\mathrm{iso}}(\mathrm{N}_i) = \frac{8\pi}{3}P_{\mathrm{N}}(\rho_{1\mathrm{s}}^{\mathrm{N}_i}|\varphi_{1\mathrm{s}}^{\mathrm{N}_i}(\vec{R}_{\mathrm{N}_i})|^2 + \rho_{2\mathrm{s}}^{\mathrm{N}_i}|(\vec{R}_{\mathrm{N}_i})|^2 + 2\rho_{1\mathrm{s}2\mathrm{s}}^{\mathrm{N}_i}\varphi_{1\mathrm{s}}^{\mathrm{N}_i}(\vec{R}_{\mathrm{N}_i})\varphi_{2\mathrm{s}}^{\mathrm{N}_i}(\vec{R}_{\mathrm{N}_i})) \quad (11d)$$

where the subscripts π_{ip} and π_{op} refer to the in-plane and out-of-plane π-orbitals on the nitrogen ligands. Clearly, $A_{\pi_{\mathrm{ip}}}(N_i)$ only for $\rho_{\pi_{ip}} = \rho_{\pi_{op}}$. If Ψ_S^M is approximated by the ROHF-LCAO-MO procedure,[63] the spin density $D_S(\vec{r})$ is solely determined by the SOMO ($\rho_{ij} = c_{i,\mathrm{SOMO}}\, c_{j,\mathrm{SOMO}}$). For sufficiently high symmetry (i.e., D_{4h}), there is no mixing between σ- and π-orbitals ($\rho_{\pi_{\mathrm{ip}}} = \rho_{\pi_{\mathrm{op}}} = 0$). If furthermore the spin polarization of the nitrogen 1s orbital is negligible, the familiar equations are recovered:[60−62]

$$A_{||}(\mathrm{N}_i) = A_\sigma(\mathrm{N}_i) = \rho_{2\mathrm{s}}A_{\mathrm{s}} + \frac{4}{5}\rho_{2\mathrm{p}}A_{\mathrm{p}} \quad (12a)$$

$$A_\perp(\mathrm{N}_i) = A_\pi(\mathrm{N}_i) = \rho_{2\mathrm{s}}A_{\mathrm{s}} - \frac{2}{5}\rho_{2\mathrm{p}}A_{\mathrm{p}} \quad (12b)$$

where $A_{\mathrm{s}} \equiv (8\pi/3)P_N|\varphi_{2\mathrm{s}}^{N_i}(\vec{R}_{\mathrm{N}_i})|^2$, $A_{\mathrm{p}} \equiv P_N\langle r^{-3}\rangle_{N2\mathrm{p}}$ and the MOs are written as $\phi_i(\vec{r}) = \sum_A\sum_j^A c_{ji}\varphi_j^A(\vec{r})$.

The value R is defined as $R \equiv A_{||}^{\mathrm{N}}/A_\perp^{N}$.[64] A theoretical expression for $\rho_{2s}/\rho_{2\mathrm{p}}$ in terms of R is readily obtained from eq 12:

$$\frac{\rho_{2\mathrm{s}}}{\rho_{2\mathrm{p}}} = \frac{2}{5}\frac{A_{\mathrm{p}}}{A_{\mathrm{s}}}\left(\frac{R+2}{R-1}\right) \quad (13)$$

Equation 13 is usually used to infer $\rho_{2s}/\rho_{2\mathrm{p}}$ from the measured value of R.[65]

For the situation where $\rho_{\pi_{\mathrm{ip}}} = \rho_{\pi_{\mathrm{op}}} = \rho_\pi$ it is seen from eq 11 that the right-hand side of eq 13 is equal to $\rho_s/(\rho_\sigma - \rho_\pi)$. An equation for $\rho_\pi/\rho_{\mathrm{s}}$ can then be derived:

$$\frac{\rho_\pi}{\rho_{\mathrm{s}}} = \frac{\rho_\sigma}{\rho_{\mathrm{s}}} - \frac{5}{2}\frac{A_{\mathrm{s}}}{A_{\mathrm{p}}}\left(\frac{R-1}{R+2}\right) \text{ or } \frac{\rho_\pi}{\rho_\sigma} = 1 - \frac{5}{2}\frac{A_{\mathrm{s}}}{A_{\mathrm{p}}}\frac{\rho_{\mathrm{s}}}{\rho_\sigma}\left(\frac{R-1}{R+2}\right) \quad (14)$$

In the ideal sp^n hybridization case $\rho_\sigma/\rho_{\mathrm{s}} = n$. However, the calculations described in section 4 indicate that this is only a rough estimate, and that the actual ratio may be between n and $n+1$. For example, in $[Cu(NH_3)_4]^{2+}$, the calculated $\rho_\sigma/\rho_{\mathrm{s}}$ is 3.30 compared to 3.00 expected from sp^3 hybridization. The measured R for this complex is 1.23.[61] Using $A_{\mathrm{s}}/A_{\mathrm{p}} = 13.21$[66] a value of $\rho_\sigma/\rho_{\mathrm{s}} = 0.94$ is obtained with the calculated $\rho_\sigma/\rho_{\mathrm{s}}$ and 0.65 with the ideal $\rho_\sigma/\rho_{\mathrm{s}}$ of 3.00. This is not to say that NH_3 forms π-bonds with Cu(II), but is an estimate of the spin polarization of the N−H bonds by the unpaired spin on the nitrogen atom in this complex. The total spin density on nitrogen is then readily obtained if ρ_{s} is known from the solution spectrum or from the trace of the measured hyperfine tensor. The numbers will depend on the values used for A_{s}, A_{p}, and ρ_σ/ρ_s. Using $\rho_\sigma/\rho_{\mathrm{s}} = 3.30$ in the case of $[Cu(NH_3)]^{2+}$ the total nitrogen spin density is 11.5% compared to 10.3% with $\rho_\sigma/\rho_{\mathrm{s}}$

TABLE 1: Calculated (INDO/S) and Observed HFCs (in MHz) and Spin Densities for a Variety of Cu(II) Complexes: The Tabulated Values Are the Square Root of the Eigenvalues of A^TA, and Abbreviations Used for Ligands Are Gly = Glycine, en = Ethylenediamine, iz = Imidazole, py = Pyridine

compound	method	ρ_{2s}[a]	ρ_σ	ρ_π	A_{iso}[b]	$A_{\|\|}$[d]	$A_\perp$[d]	R	ρ_N[c]
$[Cu(NH_3)_4]^{2+}$	INDO/S−UHF	0.023	0.076	0.010	35.0	42.6	31.7	1.34	0.109
	INDO/S−ROHF	0.018	0.065	0.000	26.0	32.0	22.8	1.40	0.081
	exptl[61] [e]	0.022	0.067−0.078	0.014−0.026	34.2	39.1	31.7	1.23	0.103−0.125
$[Cu(gly)_2]^0$	INDO/S−UHF	0.018	0.055	0.007	27.3	32.1	24.9	1.28	0.080
	INDO/S−ROHF	0.011	0.051	0.000	18.2	23.0	15.7	1.46	0.062
	exptl[61] [e]	0.020	0.061−0.072	0.015−0.025	31.5	35.8	29.3	1.22	0.097−0.117
$[Cu(en)_2]^{2+}$	INDO/S−UHF	0.023	0.080	0.009	34.6	41.6	31.0	1.34	0.113
	INDO/S−ROHF	0.014	0.073	0.000	22.3	29.4	18.8	1.56	0.088
	exptl[61] [e]	0.020	0.075−0.090		31.5	39.4	27.6	1.43	
$[Cu(iz)_4]^{2+}$	INDO/S−UHF	0.030	0.045	0.010	45.1	48.9	42.4	1.15	0.085
	INDO/S−ROHF	0.022	0.052	0.000	34.1	39.2	31.4	1.25	0.074
	exptl[61] [e]	0.026	0.052−0.066	0.037−0.050	40.4	41.6	39.8	1.05	0.116−0.142
$[Cu(py)_4]^{2+}$	INDO/S−UHF	0.030	0.058	0.011	45.8	50.7	43.1	1.18	0.099
	INDO/S−ROHF	0.022	0.068	0.000	34.7	41.2	31.4	1.31	0.089
	exptl[61] [e]	0.024	0.051−0.065	0.022−0.035	40.0	41.3	34.8	1.11−1.19	0.099−0.125

[a] "Experimental" values refer to $A_{iso}/1540$. [b] Experimental values for A_{iso} were estimated by $(^1/_3)(A_{||} + 2A_\perp)$. [c] ρ_N is the total spin density on any of the nitrogen ligands. [d] Where the calculated hyperfine tensor was rhombic A_{min} and A_{mid} were averaged to give $A_\perp$. [e] Only the experimental values for $A_{||}$, $A_\perp$, and R are taken from ref 61. All other values are inferred from this work.

= 3.00. Thus, this analysis suggests that ≈17−20% of the total spin density on nitrogen is in the nitrogen out-of-plane orbitals.

4. Calculations

4.1. Semiempirical Calculations. Semiempirical UHF- and ROHF−INDO/S calculations[67] were carried out for the range of compounds which were studied experimentally by Scholl and Hüttermann[61] in order to obtain more insight into the nitrogen HFCs discussed in the previous section. In the UHF calculation the spin density matrix is given by[68]

$$\rho_{ij} = \sum_k n_k^\alpha c_{ik}^\alpha c_{jk}^\alpha - n_k^\beta c_{ik}^\beta c_{jk}^\beta \qquad (15)$$

where n_i^α and n_i^β are occupation numbers and the MO coefficients c_{ik}^α and c_{ik}^β are determined by the self-consistent field (SCF) procedure. Equation 15 is the lowest level of theory at which the experimental results can be satisfactory explained, since it does not constrain the out of plane spin density components to be zero, i.e., the spin polarization of the N−R bonds and the nitrogen core is allowed for.

The agreement of the UHF−INDO/S HFCs in Table 1 and the experimental values of ref 61 are quite good for "sp^3-nitrogens" but less satisfying for "sp^2-nitrogens", where the calculated couplings are too large mainly due to the overestimation of the isotropic part. The HFCs calculated by the ROHF method are consistently smaller than the UHF values. The R values calculated by the UHF−INDO/S method are always smaller than the ROHF-values and are in better agreement with the experimental data.[61] As can be seen from the orbital spin populations in Table 1 the origin of this effect is indeed the spin polarization of the N−R bonds, i.e., the introduction of spin density in the nitrogen π-orbitals which counteracts the dipolar contributions of the nitrogen σ-donor orbital. However, the UHF−INDO/S R values are still too large, which suggests that the spin polarization may even be slightly underestimated by this method.

4.2. Density Functional Calculations. *4.2.1. Functional Dependence.* The dependence of the nitrogen HFCs on the approximate density functional was also studied for $[Cu(NH_3)_4]^{2+}$. The results in Table 2 show that the functionals basically divide into two groups. The hybrid functionals, that involve part of the HF exchange and the pure density functionals without such terms.

TABLE 2: Dependence of the Computed Nitrogen HFCs of $[Cu(NH_3)_4]^{2+}$ on the Approximate Density Functional (Cu−N Bondlength = 2.05 Å)[a]

method	A^{iso} (MHz)	A_1 (MHz)	A_2 (MHz)	A_3 (MHz)
Hartree−Fock	22.8	20.4	20.4	27.5
B3LYP	37.8	32.7	32.7	47.9
B1LYP	37.2	32.3	32.4	46.9
PBE0	37.8	32.8	32.9	47.7
PWP1	34.3	29.7	29.8	43.4
BP	40.5	34.8	34.9	51.9
GP	41.7	35.8	35.9	53.5
BLYP	40.4	34.7	34.8	51.8
PBE	41.2	35.2	35.3	53.2
PWP	36.9	31.7	31.7	47.2
exptl	34.2	31.7	31.7	39.1

[a] A_1−A_3 are the principal elements of the full hyperfine tensor ($\mathbf{A} = \mathbf{A}_1^{iso} + \mathbf{A}^{aniso}$)

The HF method itself may be regarded as a special case of DFT in which the exchange is treated exactly and correlation is completely neglected.[70] Clearly, the HF predictions for the nitrogen HFCs are poor (Table 2). The predicted values for both the isotropic and the anisotropic parts are much too small. This can be traced back to a strongly underestimated spin density on the nitrogen ligand that is due to the overestimation of bond ionicity in polar bonds by the Hartree−Fock method.[71]

In general, the hybrid functionals give smaller values for both, the isotropic as well as the anisotropic part of the nitrogen HFC compared to the pure density functionals. As the values predicted by the hybrid functionals are already slightly larger than the experimental values (tables 2,3), it is concluded that they are more suitable for the prediction of nitrogen HFCs in Cu(II) complexes. This observation is consistent with the idea that the GGA functionals overestimate the covalency of the copper−nitrogen bonds. It is perhaps not surprising, that admixture of a certain amount of exact exchange corrects the pure DFT picture in direction of the HF results, i.e., more ionic bonds. In general, the GGA functionals give Mulliken spin-populations on the nitrogens that are 15−30% larger than those calculated with the hybrid functionals. The various hybrid functionals tested behave rather similarly. The values produced by the B3LYP method are therefore representative of all these functionals. Noticeably different values are only produced by the PWP1 hybrid functional that give a very good prediction for the isotropic nitrogen HFC in $[Cu(NH_3)_4]^{2+}$. However, like all other

TABLE 3: Mulliken Spin Densities and Comparison of Computed and Experimentally Determined Nitrogen HFCs for Several Cu(II) Complexes

complex	method	ρ^N_{total} (%)	ρ^N_s (%)	ρ^N_p (%)	A^N_{iso} (MHz)	A^N_{dip} (MHz)	$A^N_{||}$ (MHz)	$A^N_{\perp}$ (MHz)	R
$[Cu(NH_3)_4]^{2+}$	B3LYP	11.2	1.53	9.7	37.8	12.7	47.9	32.7	1.47
	PWP1	9.6	1.29	8.3	34.3	11.4	43.4	29.7	1.46
	exptl				34.2	6.2	39.1	31.7	1.23
$[Cu(gly)_2]^0$	B3LYP	9.6	1.38	8.2	36.2	11.7	45.6	31.6	1.44
	PWP1	8.5	1.17	7.4	33.9	10.8	42.6	29.6	1.44
	exptl				31.5	5.4	35.8	29.3	1.22
$[Cu(en)_2]^{2+}$	B3LYP	11.6	1.47	10.1	32.2	13.8	43.3	26.8	1.62
	PWP1	10.0	1.21	8.8	28.8	12.3	38.7	23.9	1.62
	exptl				31.5	5.4	35.8	29.3	1.22
$[Cu(iz)_4]^{2+}$	B3LYP	8.8	2.53	6.2	46.6	8.2	54.8	42.5	1.29
	PWP1	8.3	2.13	6.2	43.4	8.1	51.5	39.4	1.31
	exptl				40.4	1.5 (?)	41.6	39.8	1.05
$[Cu(py)_4]^{2+}$	B3LYP	11.2	2.34	8.9	47.4	12.1	57.0	42.6	1.34
	PWP1	9.0	1.97	7.0	41.4	11.3	50.5	36.8	1.37
	exptl				40.0	5.4	41.3	34.8	1.11−1.19

functionals, it also overestimates the dipolar contribution to the nitrogen HFC.

In summary, it appears that hybrid DFT methods are the most successful for the prediction of nitrogen HFCs in Cu(II) complexes. Among the hybrid functionals, the B3LYP and PWP1 methods were chosen for the remaining calculations.

4.2.2. Results for Representative Copper Complexes. In this section the calculations are extended to a range of copper complexes that have been studied experimentally by ENDOR spectroscopy.[61] It is noted that the PWP1 functional leads to systematically slightly smaller spin densities on the ligands than the B3LYP functional and therefore also to slightly smaller predicted HFCs (Table 3). In general, the predictions from PWP1 for the isotropic HFC are better than those from the B3LYP functional that are systematically too high by 10−20%. The predictions of the PWP1 functional show an error that is uniformly smaller than 10%. It should, however, be noted that the experimental values for the isotropic HFC constants critically depend on the experimental values of $A^N_{||}$ and $A^N_{\perp}$. Thus, any error in these values will directly show up as an error in A^{iso}.

The predictions for the spin dipolar part of the HFCs are less satisfactory. Here both the PWP1 and the B3LYP functional predict values that are too large by about a factor of 2. Therefore, as a net result, the B3LYP functional leads to predicted HFCs with a value much too large for $A^N_{||}$ because it overestimates both A^{iso} and A^N_{dip}. The error for $A^N_{\perp}$ from the B3LYP calculations is acceptable. However, this is a fortuitous agreement because the overestimation of A^{iso} and the negative contribution from the strongly overestimated A^N_{dip} approximately cancel. The situation is better for the PWP1 functional that overestimates $A^N_{||}$ and underestimates $A^N_{\perp}$ due to the overestimation of A^N_{dip}. Since the error in this functional appears to be fairly systematic one could attempt to obtain better predictions by scaling the dipolar part of the predicted HFCs by a factor of ≈0.5.

Another consequence of the imbalance between the isotropic and anisotropic parts of the nitrogen HFCs from B3LYP and PWP1 is that they both overestimate the ratio $R = A^N_{||}/A^N_{\perp}$. This is a direct consequence of predicting too large values for the dipolar coupling. Both B3LYP and PWP1 behave similar in this respect.

In summary, the isotropic nitrogen HFCs predicted by the PWP1 functional are in good agreement with the experimental values while the B3LYP functional overestimates these couplings by 10−20%. Both functionals overestimate the dipolar contribution to the nitrogen HFC by about a factor of 2.

4.2.3. One-, Two-, and Three-Center Contributions to the Hyperfine Couplings. In this section, the importance of the various contributions to the individual parts of the HFCs were calculated for $[Cu(NH_3)_4]^{2+}$ (eqs 8−10). It can be seen from the data in Table 4 that the local contributions (one-center terms) dominate both the isotropic and the anisotropic part of the nitrogen HFC and the three-center terms are negligible. However, the dominance of the local contributions is not as strong as might have been anticipated. For both the isotropic and the anisotropic part of the nitrogen HFCs the two center contributions reach 10% of the final values.

TABLE 4: One-, Two-, and Three-Center Contributions to the Calculated HFCs in $[Cu(NH_3)_4]^{2+}$ Using the B3LYP Functional

	A^N_{iso} (MHz)	A^N_{max} (MHz)	$A_{mid}{}^N$ (MHz)	$A_{min}{}^N$ (MHz)
1-center	34.96	−4.93	−4.95	9.87
2-center crystal field	−0.02	−0.68	−0.53	1.21
2-center bond	2.76	+0.47	+0.45	−0.91
3-center	0.06	<0.01	<0.01	<0.01
total	37.76	−5.09	−5.03	10.12

In the case of the isotropic HFC the two-center "crystal-field" contributions are genuine distant contributions and are very small. However, the "bond" terms, where one function is located on the atom of interest and one function on a neighboring atom (eq 8b), is relatively large. In the case of square planar Cu(II) complexes with nitrogen donors this effect can be traced back to the influence of the nearby Cu(II) ion. The metal has most of the spin density in the $d_{x^2-y^2}$ orbital that has a nonzero amplitude at the position of the nitrogen nucleus (compare inset of Figure 1) and therefore contributes to the isotropic nitrogen HFC.

For the anisotropic part the one-center terms are much closer to the final values. From Table 4 it is seen that this is a consequence of a nearly complete cancellation of the two-center "bond" (eq 9a) and "crystal-field" (eq 9b) contributions that are of different sign and similar magnitude. In the general case one should, however, probably not rely on such a cancellation. Note that at larger distances the "bond" contributions rapidly become negligible because the basis function overlap decays exponentially. The "crystal-field" contributions are of longer range because they only decay as an odd inverse power of the nucleus in question to the spin carrying center. This is the basis for the success of the point−dipole approximation to this term, which is frequently used in the analysis of ENDOR data to estimate proton HFCs from a known structure or conversely to estimate the intercenter distance from the measured HFCs.[3,59]

In summary, the results of this section show that the nitrogen HFCs are dominated to ≈90% by the local contributions from

basis functions that are centered on the nitrogen atom in question. Two-center terms should be taken into account in a quantitative analysis and the three center terms can be safely ignored.

4.2.4. Relativistic Effects on the Nitrogen Hyperfine Coupling. To estimate the importance of relativistic effects on the nitrogen HFCs, these effects were studied for the prototype $[Cu(NH_3)_4]^{2+}$ complex. The scalar relativistic effects were taken into account within the ZORA framework as implemented in the ADF program.[45] Spin polarized all electron calculations with a reasonably large STO basis set and the BP functional were carried out as described in section 2.3 with and without the inclusion of scalar relativistic effects.[72] Importantly, the inclusion of the scalar relativistic effects led to changes in the computed nitrogen HFCs on the order of $\approx$0.1 MHz which is well below the geometry and basis set effects. Scalar relativistic effects are therefore seen to have negligible influence on the conclusions drawn here.

Unfortunately The spin−orbit coupling effects cannot presently be estimated from spin polarized ZORA calculations.[23] Therefore, conventional uncoupled perturbation theory[73] within the Kohn−Sham DFT framework was used to roughly estimate these effects. For the spin polarized case, the following approximate equation was implemented in the program ORCA:[74]

$$A_{\mu\nu}^{\mathrm{orb}}(\mathrm{N}) = P_{\mathrm{N}} \sum_{\sigma=\alpha,\beta} (-1)^{\delta_{\sigma\beta}} \sum_{j_\sigma} \sum_{b_\sigma} \left[\frac{2\langle \psi_j^\sigma | r_{\mathrm{N}}^{-3} l_\mu^{\mathrm{N}} | \psi_b^\sigma \rangle \langle \psi_b^\sigma | \sum_A \xi(r_{\mathrm{A}}) l_\nu^A | \psi_j^\sigma \rangle}{\epsilon_j^\sigma - \epsilon_b^\sigma} + \sum_{\rho,\tau=x,y,z} i\bar{\epsilon}_{\rho\tau\mu} \frac{\langle \psi_j^\sigma | \sum_A \xi(r_{\mathrm{A}}) l_\rho^A | \psi_b^\sigma \rangle \langle \psi_b^\sigma | \hat{F}_{\tau\nu}(\mathrm{N}) | \psi_j^\sigma \rangle}{\epsilon_j^\sigma - \epsilon_b^\sigma} \right] \quad (16)$$

In eq 16 ψ_j^σ refers to occupied Kohn−Sham orbitals of spin σ and ψ_b^σ to virtual Kohn−Sham orbitals of spin σ with orbital energies ϵ_j^σ and ϵ_b^σ, respectively. For the spin−orbit coupling operator, an effective one-electron operator, $\xi(r_{\mathrm{A}})$, was used that has been parametrized and tested with good success by Koseki et al.[75,76] The operator l_μ^A is the μth component of the angular momentum operator relative to center A. $\bar{\epsilon}_{\rho\tau\mu}$ is the antisymmetric Levi-Civitta symbol, the sum A is taken over all nuclei and N is the nucleus the HFC is calculated for.

From eq 16 it is expected that the orbital contribution to the metal hyperfine coupling will be large due to the large spin−orbit coupling in the vicinity of the metal nucleus and the small energy denominators that arise from the low lying d−d excitations. However, for light ligand nuclei (C,N,O) a much smaller effect is expected due to their small spin−orbit coupling and the larger energy gaps in the denominator. This expectation is confirmed by the numerical calculations with the BP functional where the numerically largest contribution to the nitrogen HFC in $[Cu(NH_3)_4]^{2+}$ was found to be $\approx$0.13 MHz. Thus, the spin−orbit effect can also be regarded as negligible for the purpose of the present study.[78]

4.2.5. Approximate One-Center Parameters from the DFT Calculations. To obtain more insight into the origin of the nitrogen HFCs and the assumptions made in the semiempirical calculations, the relation of the calculated values to the traditional one-center parameters was examined. The one-center parameters are the quasi-atomic isotropic HFC and the effective $\langle r^{-3}\rangle_{2\mathrm{p}}$ value for nitrogen. If these parameters were strictly transferable, a simple multiplication of the spin density with these quasi-atomic values would directly yield the HFCs. The values commonly used are 1540 MHz for A_{iso}^N and 3.02 au^{-3} $\langle r^{-3}\rangle_{2\mathrm{p}}$ (section 2.6).

Using the data in Table 3 it is seen that the correlation between the calculated isotropic HFC and the s-orbital spin density is poor. Quasi-atomic couplings predicted from these data would vary between 1800 and 2700 MHz. The reason for this is, that the total s-orbital spin population does not take into account which basis functions contribute to it. Different basis functions have grossly different amplitudes at the position of the nitrogen nucleus. In different chemical environments different basis functions will be selected for bonding and therefore there are large variations in the physical spin density at the nitrogen nucleus even though the value for $\rho_{2\mathrm{s}}^N$ may not change much. All that physically matters is the physical spin density $D_{\mathrm{S}}(\vec{R}_N)$ and not the parts that contribute to it. The lack of transferability in the calculated DFT values does not prove, however, that there is no transferability in the hyperfine parameters as such. The relatively good agreement between the semiempirical values and the measured couplings would argue that some transferability indeed exists and transferability arguments have been used for a long time with success in organic chemistry. What can be concluded is that the Mulliken s-orbital spin density from DFT calculations is a poor guide to the actual isotropic HFCs.

For the anisotropic part of the nitrogen hyperfine tensor the transferability is better. Dividing A_{dip}^N by ρ_{p}^N gives a quasi-atomic value of 135 ± 7 MHz which translates into an effective $\langle r^{-3}\rangle_{2\mathrm{p}}$ of about 3.5 au^{-3} which is slightly larger than the atomic values that are 3.2 au^{-3} for the neutral N atom and 2.65 au^{-3} for the negative ion using the same methods and basis sets.

In summary it is found, that the *calculated* values of $|\varphi_{2\mathrm{s}}(0)|^2$ are not transferable from the isolated nitrogen atom to nitrogen atoms bonded in complexes. Thus, the Mulliken spin density $\rho_{2\mathrm{s}}$ cannot be used to predict the isotropic coupling but the physical spin density $D_S(\vec{R}_N)$ needs to be evaluated. The values predicted by the DFT calculations for $D_S(\vec{R}_N)$ appear to be of reasonable quality in the complexes studied as judged from the agreement of the isotropic HFC predictions. The transferability of $\langle r^{-3}\rangle_{2\mathrm{p}}$ is better. Here the DFT calculations predict an effective value that is larger than that calculated for the isolated atom.

5. Discussion

In this work the ligand HFCs that are prominently observed in magnetic resonance spectra of Cu(II) complexes with nitrogen donors were studied theoretically and computationally using semiempirical and DFT approaches.

In the DFT calculations good agreement with experimental data is only found for the isotropic HFCs and only if hybrid functionals such as B3LYP and PWP1 are used. The anisotropic HFCs are consistently overestimated by about a factor of 2 by all functionals. GGA functionals lead to consistently worse agreement with experiment and overestimate both, the isotropic and the anisotropic nitrogen HFCs. This is consistent with the idea that such functionals tend to overestimate the covalencies of metal−ligand bonds. An effort was undertaken to eliminate technical factors that could obscure the interpretation of this result. These factors include basis set effects, geometry effects, multicenter contributions and the scalar relativistic and spin−orbit coupling corrections. All of these factors are estimated to be smaller than the remaining disagreement with the experimental results. One factor that was not studied in the present work is the effect of the molecular environment such as crystal

packing and solvation effects. While these effects are not envisioned to be large, they cannot be eliminated as a significant source of error. With this caveat in mind, the results of this work indicate that the main source of disagreement between theory and experiment is in the density functionals themselves.

On the basis of the analysis in section 3, the spin polarization of the valence shell is expected to significantly influence the prediction of the nitrogen HFCs studied in this work. This is particularly evident in the semiempirical results that only show good agreement with the experimental data if the calculations are performed in the spin-unrestricted scheme. However, in view of the approximations involved in the semiempirical treatment, the good agreement may be slightly fortuitous. It is nevertheless difficult to explain the small values of $A_{||}^N/A_{\perp}^N$ observed experimentally without recourse to spin polarization. This has important consequences for the interpretation of EPR and ENDOR data for complexes of the type studied here. While the bonding in the complexes under investigation may well be rationalized in terms of sp^2 and sp^3 hybrid orbitals, the spin density distribution is not well described by these concepts, due to the spin polarization of the adjacent N−H and N−C bonds. Consequently, the estimation of nitrogen MO coefficients in the SOMO from experimental data alone can lead to significant errors. A closely related conclusion was drawn by Munzarova and Kaupp (MK) in their detailed studies of metal HFCs.[18,20] Indeed, MK stated that "the widely used simplified models that derive the d- or s-character of the SOMO directly from the dipolar coupling constants should be viewed with caution in transition metal systems".[18] Thus, the interpretation of superhyperfine structure in transition metal complexes appears to be more subtle than is frequently assumed. We also note in passing that in general it is not valid to compare experimentally determined spin populations to those from a Mulliken population analysis of the spin density matrix as is often done. The latter values contain overlap terms but the former are usually derived under the one-center approximation where only the diagonal terms of the spin-density matrix contribute to the HFCs.

One possibility for the relatively poor performance of the DFT methods for the anisotropic nitrogen couplings is that the spin polarization of the valence shell is underestimated by the functionals used. The importance of spin polarization for the interpretation of HFCs was also pointed out by Belanzoni et al.[24,25] in their careful study of TiF_3 and investigated in detail by MK.[18] The latter authors concluded that none of the present functionals behaved uniformly satisfactory in this respect. In the compounds studied by MK, the experimentally available ligand dipolar couplings were either small or no experimental data was available such that detailed comparison with experiments was not feasible. An exception is $Cu(CO)_3$ for which most functionals, including B3LYP, gave good agreement with experiment.[18] For TiF_3 Belanzoni et al.[24,25] have obtained excellent agreement for the parallel component of the fluorine HFC that appears to be dominated by the dipolar coupling. The splitting in the perpendicular region was calculated too large with the BP functional and the observed HFC remained not completely understood. Van Lenthe et al. studying the same system, obtained good overall agreement with the results of Belanzoni et al.[23] In addition they computed small scalar relativistic corrections but spin−orbit corrections of up to 20% for the dipolar fluorine couplings.[23] In the study by Hayes[27] on $[Ni(mnt)_2]^-$ various DFT functionals overestimated the dipolar couplings for sulfur. Better values were obtained for carbons and nitrogens, but the observed dipolar couplings were very small (<1 MHz). It would be interesting to explore in systematic studies whether the overestimation of dipolar HFCs by DFT methods found in this work is a more general feature or if it is peculiar to the Cu(II) compounds studied here. Also, the importance of relativistic corrections for the prediction of ligand hyperfine structure should be assessed for a larger set of transition metal complexes in different bonding situations.

In any case we agree with Munzarova and Kaupp[18] and with Schreckenbach[79] that for the future design of new functionals it would be desirable if spectroscopic properties would be included in the training set. HFCs in transition metal complexes are very sensitive to the quality of the exchange correlation *potential*. In addition, they provide a wide variety of bonding situations ranging from mostly ionic to mostly covalent bonding and a wide range of different spin states and spin polarization situations. HFCs should therefore provide critical test cases for newly developed functionals. It would also be desirable to base the developments not only on the exchange-correlation energies but also on the exchange-correlation potential. A point of concern is the observation by van Leeuwen and Baerends that the present day functionals have not only the wrong asymptotic behavior in the long range but also close to the nucleus where they show an unphysical divergence.[80] This is expected to have important consequences for the prediction of isotropic hyperfine couplings.

For the time being, hybrid DFT calculations (B3LYP and/or PWP1) can be used to predict and interpret ligand hyperfine structure in large Cu(II) complexes within reasonable calculation times. However, the deficiencies of this method should be kept in mind and may be empirically corrected because they appear to be fairly systematic.

Acknowledgment. Financial support of this work by Deutsche Forschungs-gemeinschaft and the Fonds der Chemischen Industrie is gratefully acknowledged. I thank several members of the computational chemistry mailing list (CCL) for helping to resolve a technical problem with the field gradient integrals and Prof. Peter Kroneck (Konstanz) for his support and encouragement.

Supporting Information Available: Basis set (Table S1) and geometry dependence (Table S2) of the computed nitrogen HFC's for $[Cu(NH_3)_4]^{2+}$. This material is available free of charge via the Internet at http://pubs.acs.org.

References and Notes

(1) Holm, R. H.; Kennepohl, P.; Solomon, E. I. *Chem. Rev.* **1996**, *96*, 2239.

(2) Abragam, A.; Bleaney, B. *Electron Paramagnetic Resonance of Transition Ions*; Dover Publishers, Inc.: New York, 1970.

(3) (a) Hoffman, B. M.; DeRose, V. J.; Gurbiel, R. J.; Houseman, A. L. P.; Telser, J. In *Biological Magnetic Resonance, Volume 13: EMR of Paramagnetic Molecules*; Berliner, L. J., Reuber, J., Eds.; Plenum Press: New York, 1993; p 151. (b) Hüttermann, J. In *Biological Magnetic Resonance, Volume 13: EMR of Paramagnetic Molecules*; Berliner, L. J., Reuber, J., Eds.; Plenum Press: New York, 1993; p 219. (c) Schweiger, A. *Electron Nuclear Double Resonance of Transition Metal Complexes with Organic Ligands*; Springer-Verlag: NewYork, 1982. (d) Gemperle, C.; Schweiger, A. *Chem. Rev.* **1991**, *91*, 1481. (e) Lowe, D. J. *ENDOR and EPR of Metalloproteins*; Springer: New York, 1995.

(4) (a) McGarvey, B. R. In *Transition Metal Chemistry*; Carlin, R. L., Ed.; Marcel Dekker: New York, 1966; Vol. 3, p 89. (b) Neese, F.; Solomon, E. I. *Inorg. Chem.* **1998**, *37*, 6568.

(5) Solomon, E. I. *Comments Inorg. Chem.* **1984**, *3*, 227.

(6) (a) Hedman, B.; Hodgson, K. O.; Solomon, E. I. *J. Am. Chem. Soc.* **1990**, *112*, 1643. (b) Neese, F.; Hedman, B.; Hodgson, K. O.; Solomon, E. I. *Inorg. Chem.* **1999**, *38*, 4854.

(7) For reviews, see: (a) Hathaway, B. J.; Billing, D. E. *Coord. Chem. Rev.* **1970**, *5*, 143. (b) Hathaway, B. J.; *Coord. Chem. Rev.* **1983**, *52*, 87.

(8) (a) Maki, A. H.; McGarvey, B. R. *J. Chem. Phys.* **1958**, *29*, 31. (b) *J. Chem. Phys.* **1958**, *35*. Also see: (c) Gewirth, A. A.; Cohen, S. L.; Schugar, H. J.; Solomon, E. I. *Inorg. Chem.* **1987**, *26*, 1133. (d) Penfield, K. W.; Gewirth, A. A.; Solomon, E. I. *J. Am. Chem. Soc* **1985**, *107*, 4519.

(9) Kivelson, D.; Neimann, R. *J. Chem. Phys.* **1961**, *35*, 149.

(10) Ammeter, J. *Chimia*, **1968**, *22*, 469.

(11) For recent reviews, see: (a) *Chem. Rev.* **2000**, *100*. (b) Schleyer, P. v. R., Allinger, N. L., Clark, T., Gasteiger, J., Kollman, P. A., Schaefer, H. F., III, Schreiner, P. R., Eds. *Encyclopedia Computational Chemistry*; John Wiley and Sons Ltd: Chichester, England, 1998.

(12) (a) Roos, B. O. In *Ab Initio Methods in Quantum Chemistry-II*; Lawley, K. P., Ed.; John Wiley & Sons: New York, 1992; p 399ff. (b) Bauschlicher, C. W. In *Encyclopedia Computational Chemistry*; Schleyer, P. v. R., Allinger, N. L., Clark, T., Gasteiger, J., Kollman, P. A., Schaefer, H. F., III, Schreiner, P. R., Eds.; John Wiley and Sons Ltd: Chichester, England, 1998; p 3084ff.

(13) Solomon, E. I.; Baldwin, M. J.; Lowery, M. D.*Chem. Rev.* **1992**, *92*, 521. (b) Swann, J.; Westmoreland, T. D. *Inorg. Chem.* **1997**, *36*, 5348.

(14) For recent reviews, see: (a) Engels, B.; Erikson, L. A.; Lunell, S. *Adv. Quantum Chem.* **1996**, *27*, 297. (b) Eriksson, L. A. In *Encyclopedia Computational Chemistry*; Schleyer, P. v. R., Ed.; John Wiley and Sons Ltd: Chichester, England, 1998; p 952. (c) Feller, D.; Davidson, E. R. In *Molecular Spectroscopy, Electronic Structure and Intramolecular Interactions*; Maksic, Z. B., Ed.; Springer-Verlag: New York, 1991; p 429. (d) Chipman, D. M. In *Quantum Mechanical Electronic Structure Calculations with Chemical Accuracy*; Langhoff, S. R., Ed.; Kluwer: Amsterdam, 1995; p 109. (e) Barone, V. In Chong, D. P., Ed. *Recent Advances in Density Functional Theory*, World Scientific: Singapore, 1995; p 287.

(15) (a) Keijzers, C. P.; DeBoer, E. *J. Chem. Phys.* **1972**, *57*, 1277. (b) Atherton, N. M.; Horsewill, A. J. *J. Chem. Soc. Faraday Discuss. 2* **1980**, *76*, 660. (c) Lupei, A.; McMillan, J. A. *J. Chem. Phys.* **1972**, *57*, 827. (d) Keijzers, C. P.; Snaathorst, D. *Chem. Phys. Lett.* **1980**, *69*, 348. (e) Larsson, S. *Theor. Chim. Acta* **1975**, *39*, 173.

(16) Keijzers, C. P.; DeBoer, E. *Mol. Phys.* **1974**, *29*, 1007.

(17) Geurts, P. J. M.; Boulen, P. C. P.; van der Avoird, A. *J. Chem. Phys.* **1980**, *73*, 1306.

(18) Munzarova, M. L.; Kaupp, M. *J. Phys. Chem. A* **1999**, *103*, 9966.

(19) Watson, R. E.; Freeman, A. *Phys. Rev.* **1961**, *123*, 2027.

(20) Munzarova, M. L.; Kubacek, P.; Kaupp, M. *J. Am. Chem. Soc.*, **2000**, *122*, 11900.

(21) van Lenthe, E.; Snijders, J. G.; Baerends, E. J. *J. Chem. Phys.* **1996**, *105*, 6505.

(22) van Lenthe, E.; Wormer, P. E. S.; van der Avoird, E. *J. Chem. Phys.* **1007**, *107*, 2488.

(23) van Lenthe, E.; van der Avoird, A.; Wormer, P. E. S. *J. Chem. Phys.* **1998**, *108*, 4783.

(24) Belanzoni, P.; Baerends, E. J.; van Asselt, S.; Langewen, P. B. *J. Phys. Chem.* **1995**, *99*, 13094.

(25) Belanzoni, P.; Baerends, E. J.; Gribnau, M. *J. Phys. Chem A* **1999**, *103*, 3732.

(26) DeVore, T. C.; Weltner, W. Jr. *J. Am. Chem. Soc.* **1977**, *99*, 4700.

(27) (a) Hayes, R. G. *Inorg. Chem.* **2000**, *39*, 156. (b) Knight, L. B.; Kaup, J. G.; Petzold, B.; Ayyad, R.; Ghanty, T. K.; Davidson, E. R. *J. Chem. Phys.* **1999**, *110*, 5658. (c) Huyett, J. E.; Choudhury, S. B.; Eichorn, D. M.; Bryngelson, P. A.; Maroney, M. J.; Hoffman, B. M. *Inorg. Chem.* **1998**, *37*, 1361.

(28) Neese, F. *ORCA−an ab initio, DFT and semiempirical program package, Version 2.0, Revison 88*; Universität Konstanz: Konstanz, Germany, 2000. Unpublished.

(29) (a) Pulay, P. *Chem. Phys. Lett.* **1980**, *73*, 393. (b) Pulay, P. *J. Comput. Chem.* **1982**, *3*, 556.

(30) (a) Dirac, P. A. M. *Proc. Cambridge. Philos. Soc.* **1930**, *26*, 376. (b) Slater, J. C. *The Quantum Theory of Atoms Molecules and Solids*; McGraw-Hill: New York, 1974; Vol. 4,

(31) Becke, A. D. *Phys. Rev. A* **1988**, *38*, 3098.

(32) Lee, C.; Yang, W.; Parr, R. G. *Phys. Rev. B.* **1988**, *37*, 785.

(33) Vosko, S. H.; Wilk, L.; Nusair, M. *Can. J. Phys* **1980**, *58*, 1200.

(34) Becke, A. D. *J. Chem. Phys.* **1993**, *98*, 5648.

(35) Adamo, C.; di Matteo, A.; Barone, V. *Adv. Quantum Chem.*, **2000**, *36*, 45.

(36) Perdew, J. P. *Phys, Rev. B.* **1986**, *33*, 8822.

(37) Perdew, J. P.; Burke, K.; Ernzerhof, M. *Phys. Rev. Lett.* **1996**, *77*, 3865.

(38) Adamo, C.; Barone, V. *J. Chem. Phys.* **1999**, *110*, 6158.

(39) Perdew, J. P.; Wang, Y. *Phys. Rev. B* **1992**, *45*, 13245.

(40) Gill, P. M. W. *Mol. Phys.* **1996**, *89*, 433.

(41) Perdew, J. P.; Chevary, J. A.; Vosko, S. H.; Jackson, K. A.; Pederson, M. R.; Singh, D. J.; Fiolhais, C. *Phys. Rev. A.* **1992**, *46*, 6671.

(42) Basis sets were obtained from the Extensible Computational Chemistry Environment Basis Set Database, Version Mon Apr 17 10: 05: 30 PDT 2000, as developed and distributed by the Molecular Science Computing Facility, Environmental and Molecular Sciences Laboratory which is part of the Pacific Northwest Laboratory, P.O. Box 999, Richland, WA 99352, U.S.A., and funded by the U.S. Department of Energy. The Pacific Northwest Laboratory is a multiprogram laboratory operated by Battelle Memorial Institue for the U.S. Department of Energy under contract DE-AC06−76RLO 1830. Contact David Feller or Karen Schuchardt for further information. http://www.emsl.pnl.gov: 2080/forms/basisform.html.

(43) Schäfer, A.; Huber, C.; Ahlrichs, R. *J. Chem. Phys.* **1994**, *100*, 5829.

(44) Godbout, N.; Salahub, D. R.; Andzelm, J.; Wimmer, E.; *Can. J. Chem.* **1992**, *70*, 560.

(45) Baerends, E. J.; Berces, A.; Bo, C.; Boerrigter, P. M.; Cavallo, L.; Deng, L.; Dickson, R. M.; Ellis, D. E.; Fan, L.; Fischer, T. H.; Fonseca Guerra, C.; van Gisbergen, S. J. A.; Groeneveld, J. A.; Gritsenko, O. V.; Harris, F. E.; van den Hoeck, P.; Jacobsen, H.; van Kessel, G.; Kootstra, F.; van Lenthe, E.; Osinga, V. P.; Phillipsen, P. H. T.; Post, D.; Pye, C. C.; Ravenek, W.; Ros, P.; Schipper, P. R. T.; Schreckenbach, G.; Snijders, J. G.; Sola, M.; Swerhone, D.; te Velde, G.; Vernoijs, P.; Versluis, L.; Visser, O.; van Wezenbeek, E.; Wolff, S. K.; Woo, T. K.; Ziegler, T. *ADF 1999*; Scientific Computing and Modelling (SCM): Amsterdam, Netherlands, 1999.

(46) Wells, A. F. *Structural Inorganic Chemistry*; 5th ed.; Oxford Clarendon Press: Oxford, 1993.

(47) McFadden, D. L.; McPhail, A. T.; Gross, P. M.; Garner, C. D.; Mabbs, F. E. *J. Chem. Soc., Dalton Trans.* **1976**, 47.

(48) Agnus, Y.; Labarelle, M.; Louis, R.; Metz, B. *Acta Crystallogr.* **1994**, *C50*, 536.

(49) Maxcy, K. R.; Turnbull, M. M. *Acta Crystallogr.* **1999**, *C55*, 1986.

(50) Freeman, H. C.; Snow, M. R.; Nitta, I.; Tomita, K. *Acta Crystallogr.* **1964**, *17*, 1463.

(51) Oxford Molecular Group *DGauss 4.1*; Oxford.

(52) Ahlrichs, R.; Bär, M.; Baron, H. P.; Bauernschmitt, R.; Böcker, S.; Ehrig, M.; Eichkorn, K.; Elliott, S.; Furche, F.; Haase, F.; Häser, M.; Horn, H.; Huber, C.; Huniar, U.; Kattanek, M.; Kölmel, C.; Kollwitz, M.; May, K.; Ochsenfeld, C.; Öhm, H.; Schäfer, A.; Schneider, U.; Treutler, O.; von Arnim, M.; Weigend, F.; Weis, P.; Weiss, H. *TurboMole−Program System for ab initio Electronic Structure Calculations*, Version 5.2; Universität Karlsruhe: Karlsruhe, Germany, 2000.

(53) McMurchie, L.; Davidson, E. R. *J. Comput. Phys.* **1978**, *26*, 218.

(54) Helgaker, T.; Taylor, P. R. In *Modern Electronic Structure Theory*; Yarkony, D., Ed.; World Scientific: Singapore, 1995; p 725.

(55) Frisch, M. J.; Trucks, G. W.; Schlegel, H. B.; Scuseria, G. E.; Robb, M. A.; Cheeseman, J. R.; Zakrzewski, V. G.; Montgomery, J. A., Jr.; Stratmann, R. E.; Burant, J. C.; Dapprich, S.; Millam, J. M.; Daniels, A. D.; Kudin, K. N.; Strain, M. C.; Farkas, O.; Tomasi, J.; Barone, V.; Cossi, M.; Cammi, R.; Mennucci, B.; Pomelli, C.; Adamo, C.; Clifford, S.; Ochterski, J.; Petersson, G. A.; Ayala, P. Y.; Cui, Q.; Morokuma, K.; Malick, D. K.; Rabuck, A. D.; Raghavachari, K.; Foresman, J. B.; Cioslowski, J.; Ortiz, J. V.; Baboul, A. G.; Stefanov, B. B.; Liu, G.; Liashenko, A.; Piskorz, P.; Komaromi, I.; Gomperts, R.; Martin, R. L.; Fox, D. J.; Keith, T.; Al-Laham, M. A.; Peng, C. Y.; Nanayakkara, A.; Challacombe, M.; Gill, P. M. W.; Johnson, B.; Chen, W.; Wong, M. W.; Andres, J. L.; Gonzalez, C.; Head-Gordon, M.; Replogle, E. S.; Pople, J. A. *Gaussian 98*, Revision A.8; Gaussian, Inc.: Pittsburgh, PA, 1998.

(56) Neese, F. Dissertation, Universität Konstanz, Konstanz, Germany, 1997.

(57) Koh, A. K.; Miller, D. J. *At. Nucl. Data Tables* **1985**, *33*, 235.

(58) (a) McWeeny, R.; Sutcliffe, B. T. *Methods of Molecular Quantum Mechanics*; Academic Press: London, 1969. (b) McWeeny, R. *Spins in Chemistry* **;** Academic Press: New York, 1970. (c) McWeeny, R. *J. Chem. Phys.* **1965**, *42*, 1717.

(59) (a) Atherton, N. M.; Shakleton, J. F. *Chem. Phys. Lett.* **1984**, *103*, 302. (b) Atherton, N. M.; Horsewill, A. J. *Mol. Phys.* **1979**, *37*, 1349. (c) Atherton, N. M.; Shakleton, J. F. *Mol. Phys.* **1980**, *39*, 1471. (d) Hutchinson, C. A.; McKay, D. B. *J. Chem. Phys.* **1977**, *66*, 3311.

(60) (a) Yordanov, N. D.; Stankova, M.; Shopov, D. *Chem. Phys. Lett.* **1976**, *39*, 174. (b) Basosi, R. *J. Am. Chem. Soc.* **1988**, *92*, 992.

(61) Scholl H. J.; Hütterman, J. *J. Phys. Chem., 96* **1992**, 9684−9691.

(62) Atherton, N. M. *Principles of Electron Spin Resonance*; Ellis Harwood Prentice Hall: New York, 1993.

(63) (a) Carbo, R.; Riera, J. A. *A General SCF Theory*; Lecture Notes in chemistry; Springer: New York, 1978. (b) Edwards, W. D.; Zerner, M. C. *Theor. Chim. Acta* **1987**, *72*, 347−361.

(64) Yokoi, H.; *Biochem. Biophys. Res. Commun.* **1982**, *108*, 1278.

(65) Note that the experimental value for R must not be obtained by using the HFCs in units of magnetic field as read from the EPR spectrum. The use of field units introduces a factor $g_{\parallel}/g_{\perp}$ in the value of R, which underestimates the term in brackets of eq 13 by up to 50%. When proper units are used, it turns out that the calculated hybridization ratios are usually larger than expected for sp^2 or sp^3 hybridization. Physically this means that the spin density distribution around the nitrogen donor is more spherical than would be suggested from the simple picture of bonding.

(66) Ayscough P. B. *Electron Spin Resonance in Chemistry*; Methuen & Co. Ltd.: London, 1967. The value $A_p = 116.5$ MHz was used which was derived with the relativistic expectation values of Desclaux (Desclaux

J. P. *At. Nucl. Data Tables* **1973**, *12*, 311) rather than $A_p = 119.5$ MHz from Table A.3 in Ayscough's book.

(67) (a) Bacon, A. D.; Zerner, M. C.; *Theor. Chim. Acta* **1979**, *53*, 21. (b) Anderson, W. P.; Edwards, W. D.; Zerner, M. C.; *Inorg. Chem.* **1986**, *25*, 2728. (c) Zerner, M. C.; Loew, G. H.; Kirchner, R. F.; Mueller-Westerhoff, U. T. *J. Am. Chem. Soc.* **1980**, *102*, 589. (d) Sedlej, J. Cooper, I. L. *Semiempirical Methods in Quantum Chemistry*; Ellis Harrwood: New York, 1985. (e) Pople, J. A.; Beveridge, D. L. *Approximate Molecular Orbital Theory*; McGraw-Hill: New York, 1970. (f) Zerner, M. C. In *Reviews in Computational Chemistry;* Lipkowitz, K. B., Boyd, D. B., Eds.; VCH: New York, 1990; Vol. 2, p 313.

(68) Pople J. A.; Nesbet R. K.; *J. Chem. Phys.* **1954**, *22*, 571.

(69) (a) Krishnan, R.; Binkley, J. S.; Seeger, R.; Pople, J. A. *J. Chem. Phys.* **1980**, *72*, 650. (b) Wachters, A. J. H.; *J. Chem. Phys.* **1970**, *52*, 1033. (c) Hay, P. J.; *J. Chem. Phys.* **1977**, *66*, 4377. (d) Raghavachari, K.; Trucks, G. W. *J. Chem. Phys.* **1989**, *91*, 1062.

(70) Parr, R. G.; Yang, W. *Density Functional Theory of Atoms and Molecules*; Oxford University Press: Oxford, 1989; Chapter 8.4.

(71) For a discussion, see, for example: Szabo, A.; Ostlund, N. S. *Modern Quantum Chemistry. Introduction to Advanced Electronic Structure Theory*; Dover Publications: Mineola, NY, 1996.

(72) It is noted that the nonrelativistic results obtained from the ADF calculations were found to be within 1 MHz of the values obtained with ORCA. We feel that this is encouraging due to the significant methodological differences in the two programs and is taken as an indication that the basis set used in this study is reasonably converged for hyperfine structure calculations.

(73) (a) Dalgarno, A.; McNamee, J. M. *J. Chem. Phys.* **1961**, *35*, 1517. (b) Langhoff, P. W.; Karplus, M.; Hurst, R. P. *J. Chem. Phys.* **1966**, *44*, 505.

(74) Equation 16 differs in a sign from eq 4 of Geurts et al.[17] but is otherwise in the same spirit and similar to the equation obtained by Keijzers and DeBoer[15a] for the spin-restricted case.

(75) Koseki, S.; Schmidt, M. W.; Gordon, M. S. *J. Chem. Phys.* **1992**, *96*, 10768. (b) Koseki, S.; Gordon, M. S.; Schmidt, M. W.; Matsunaga, N. *J. Phys. Chem.*, **1995**, *99*, 12764. (c) Koseki, S.; Schmidt, M. W.; Gordon, M. S. *J. Phys. Chem. A* **1998**, *102*, 10430.

(76) The effective nuclear charge entering Koseki's treatment are 1.0 for H, 4.55 for N, and 17.69 for copper.

(77) Malkina, O. L.; Vaara, J.; Schimmelpfennig, B.; Munzarova, M. L.; Malkin, V. G.; Kaupp, M. *J. Am. Chem. Soc.*, **2000**. *122*, 9206.

(78) The orbital contribution to the *metal* hyperfine coupling is closely related to the **g**-tensor.[8] In our approach, uncoupled DFT with the BP functional and the same spin−orbit operators underestimates **g**-shifts in the complexes studied here by a about a factor of 2 (see also the results of Malkina et al.)[77] We have confirmed for $[Cu(NH_3)_4]^{2+}$ that the uncoupled DFT calculations are still in good agreement with values obtained from the full ZORA treatment as implemented in the ADF code.[45,22] It is therefore reasonable to expect that the values obtained for the orbital contribution to the nitrogen HFC may be in error by about a factor of 2 which would still lead to the conclusion that they are negligible in the present case.

(79) Schreckenbach, G. *J. Chem. Phys.* **1999**, *110*, 11936.

(80) (a) Van Leeuwen, R.; Barends, E. J. *Phys. Rev. A* **1994**, *49*, 2421. (b) Baerends, E. J.; Gritsenko, O. V.; Van Leeuwen, R. In *Chemical Applications of Density Functional Theory*; Laird, B. B., Ross, R. B., Ziegler, T., Eds.; American Chemical Society: Washington, DC, 1996; p 20ff.